Int. J. Multiphase Flow Vol. 16, No. 5, pp. 885–897, 1990
Printed in Great Britain.

0301-9322/90 $3.00 + 0.00

THE BIOT DRAG AND VIRTUAL MASS COEFFICIENTS FOR FACE CENTERED CUBIC GRANULAR MATERIALS

B. YAVARI and A. BEDFORD

Applied Research Laboratories and Aerospace Engineering and Engineering Mechanics Department, University of Texas at Austin, Austin, TX 78712, U.S.A.

(*Received* 1 *June* 1989; *in revised form* 12 *January* 1990)

Abstract—The Biot equations model the propagation of acoustic waves in fluid-saturated porous media. The "drag" and "virtual mass" coefficients in the equations depend on the physical properties of the fluid and solid constituents, the frequency and the microstructure of the porous medium. Recently, a method has been developed for determining the drag and virtual mass coefficients as functions of frequency. The method requires solving for the motion of the fluid in the pores when the pore walls are subjected to a spatially uniform, oscillatory motion. In this work we use the finite element method to compute the fluid motion and evaluate the drag and virtual mass coefficients for granular media consisting of spherical and polyhedral grains with face centered cubic (fcc) packings. The materials we consider have porosities that range from 0.261 to 0.480. We conclude that an empirical approach based on Biot's results for cylindrical pores can adequately approximate our computations for an fcc packing of spheres.

Key Words: Biot, porous media, granular materials, finite element method

INTRODUCTION

The theory for wave propagation in a fluid-saturated porous medium developed by Biot (1956a, b) contains several coefficients which depend on the physical properties of the fluid and solid constituents, the frequency and the fabric, or microstructure, of the porous medium. Biot (1956b) determined the "drag" and "virtual mass" coefficients as functions of the frequency by assuming a straight cylindrical pore geometry. He suggested that his results could be extended to other pore geometries by prescribing two empirical parameters, the "pore size parameter" and the "tortuosity." His results were widely adopted. Subsequent authors have suggested various approaches for evaluating the pore size parameter and the tortuosity (Berryman 1980, 1981; Carman 1956; Hovem & Ingram 1979; Johnson & Plona 1982; Johnson *et al.* 1982; Ogushwitz 1985a, b; Stoll & Bryan 1969; Stoll 1974, 1977).

Bedford *et al.* (1984) proposed a method for evaluating the drag and virtual mass coefficients as functions of frequency for an arbitrary pore geometry. The method requires solving for the motion of the fluid in the pores when the pore walls are subjected to a spatially uniform, oscillatory motion. In the case of straight cylindrical pores, their method agreed with Biot's result. Bedford (1986) considered a medium consisting of alternating layers of fluid and solid. He found that when the drag and virtual mass coefficients were evaluated using the method of Bedford *et al.* (1984), the phase velocity and attenuation of the "fast" and "slow" waves predicted by the Biot theory agreed with the phase velocity and attenuation of the first and second modes of the theoretical solution for plane waves in the layered medium over a large range of frequency.

By using the finite element method to determine the motion of the fluid, the present authors (Yavari & Bedford 1988) used the method of Bedford *et al.* (1984) to determine the drag and virtual mass coefficients as functions of frequency for several two-dimensional pore spaces. We concluded that the drag coefficient is very insensitive to the pore geometry, while the virtual mass coefficient is quite sensitive to the pore geometry. We also found that our results could be expressed in nondimensional forms which permit the coefficients to be scaled for different values of a characteristic linear dimension of the pore space.

In this paper, we use the finite element method and the method of Bedford *et al.* (1984) to determine the Biot drag and virtual mass coefficients as functions of frequency for several three-dimensional pore geometries. Our approach has two elements in common with the method known as "homogenization". [See the applications of homogenization to saturated porous media

by Auriault & Sanchez-Palencia (1977), Auriault (1980) and Auriault *et al.* (1985).] We model the pore geometry as periodic, and we solve a "local problem" (the oscillatory motion of the pore fluid) to determine the coefficients.

We consider granular media consisting of face centered cubic (fcc) arrays of spherical and polyhedral grains. By altering the geometry of the polyhedral grains, we obtain the coefficients for granular media with a range of porosities. We compare our results with the values of the coefficients that have been used by other investigators.

PREVIOUS WORK

One of our objectives in carrying out this study was to evaluate the methods that previously existed for determining the drag and virtual mass coefficients in Biot's equations. To do so, we must briefly discuss the methods and some terminology. The equations obtained by Biot (1956a) for the motions of the solid and fluid constituents are

$$N\nabla^2\mathbf{u}_s + \nabla[(A+N)\nabla\cdot\mathbf{u}_s + Q\nabla\cdot\mathbf{u}_f] = \frac{\partial^2}{\partial t^2}(\rho_{11}\mathbf{u}_s + \rho_{12}\mathbf{u}_f) + b\frac{\partial}{\partial t}(\mathbf{u}_s - \mathbf{u}_f), \tag{1a}$$

and

$$\nabla[Q\nabla\cdot\mathbf{u}_s + R\nabla\cdot\mathbf{u}_f] = \frac{\partial^2}{\partial t^2}(\rho_{12}\mathbf{u}_s + \rho_{22}\mathbf{u}_f) - b\frac{\partial}{\partial t}(\mathbf{u}_s - \mathbf{u}_f). \tag{1b}$$

The terms $\mathbf{u}_s$ and $\mathbf{u}_f$ are the displacements of the solid and the fluid constituents. The coefficients A, N, Q and R govern the viscoelastic responses of the constituents. The term b is the drag coefficient. The terms ρ_{11}, ρ_{12} and ρ_{22} are mass coefficients that are related to the porosity ϕ and the densities ρ_s and ρ_f of the solid and fluid constituents by

$$\rho_{11} + \rho_{12} = (1-\phi)\rho_s \tag{2a}$$

and

$$\rho_{12} + \rho_{22} = \phi\rho_f. \tag{2b}$$

The coefficient ρ_{12} represents a "mass coupling" between the fluid and solid; Biot showed that it must be negative.

By defining the "apparent mass" or virtual mass coefficient c as

$$c = -\rho_{12} \tag{3}$$

and introducing the notation

$$P = A + 2N \tag{4}$$

into [1a,b] and [2a,b] the Biot equations can be written in the forms

$$(1-\phi)\rho_s\ddot{\mathbf{u}}_s = (P-N)\nabla(\nabla\cdot\mathbf{u}_s) + N\nabla^2\mathbf{u}_s + Q\nabla(\nabla\cdot\mathbf{u}_f) - b(\dot{\mathbf{u}}_s - \dot{\mathbf{u}}_f) - c(\ddot{\mathbf{u}}_s - \ddot{\mathbf{u}}_f) \tag{5a}$$

and

$$\phi\rho_f\ddot{\mathbf{u}}_f = Q\nabla(\nabla\cdot\mathbf{u}_s) + R\nabla(\nabla\cdot\mathbf{u}_f) + b(\dot{\mathbf{u}}_s - \dot{\mathbf{u}}_f) + c(\ddot{\mathbf{u}}_s - \ddot{\mathbf{u}}_f). \tag{5b}$$

These equations are often recast in the forms (e.g. Stoll 1974)

$$\rho\ddot{\mathbf{u}}_s - \rho_f\ddot{\mathbf{w}} = (H-N)\nabla e - C\nabla\zeta + N\Delta^2\mathbf{u}_s \tag{6a}$$

and

$$\rho_f\ddot{\mathbf{u}}_s - m\ddot{\mathbf{w}} = C\nabla e - M\nabla\zeta + \left(\frac{b}{\phi^2}\right)\dot{\mathbf{w}}, \tag{6b}$$

where

$$e = \nabla\cdot\mathbf{u}_s, \quad \mathbf{w} = \phi(\mathbf{u}_s - \mathbf{u}_f), \quad \zeta = \nabla\cdot\mathbf{w}, \quad \rho = (1-\phi)\rho_s + \phi\rho_f,$$
$$H = P + 2Q + R, \quad C = \frac{(Q+R)}{\phi}, \quad M = \frac{R}{\phi^2}, \quad m = \frac{\rho_f}{\phi} + \frac{c}{\phi^2}. \tag{7}$$

By subjecting fluid in a circular cylinder to an oscillating axial pressure gradient and calculating the resulting average velocity of the fluid and the shear stress on the wall of the pore, Biot (1956b) determined the drag coefficient b as a function of the frequency. He obtained the result

$$b = \frac{F\eta\phi^2}{k_p}, \qquad [8]$$

where η is the viscosity of the fluid, k_p is the permeability of the porous solid and

$$F = \frac{1}{4}\left[\frac{\xi T(\xi)}{1 - \left(\frac{2}{i\xi}\right)T(\xi)}\right]. \qquad [9]$$

The term $T(\xi)$ is a function of the complex Kelvin functions of the first kind and zero order and their derivatives:

$$T(\xi) = \frac{\text{ber}'(\xi) + i\,\text{bei}'(\xi)}{\text{ber}(\xi) + i\,\text{bei}(\xi)}, \qquad [10]$$

where the argument ξ is defined by

$$\xi = a_p\left(\frac{\omega\rho_f}{\eta}\right)^{1/2}; \qquad [11]$$

here ω is the frequency and a_p is the radius of the cylindrical pore. Investigators applying this result to porous media have usually treated a_p as an empirical constant called the "pore size parameter". For spherical grains, Hovem & Ingram (1979) suggested the relation

$$a_p = \phi\frac{d}{[3(1-\phi)]}, \qquad [12]$$

where d is the grain diameter.

Since the term F is complex, the drag coefficient b obtained from [8] is complex. When this complex coefficient is substituted into the equations of motion in the case of steady-state waves, the imaginary part of b effectively contributes a frequency-dependent term to the virtual mass coefficient c.

The permeability k_p of media consisting of regular grains can be approximated with the Kozeny–Carman equation (Carman 1956; Hovem & Ingram 1979):

$$k_p = \frac{\phi a_p^2}{4k_0}, \qquad [13]$$

where $k_0 = 2$ for circular tubes and $k_0 \simeq 5$ for spherical grains. The value of k_0 is given for different pore geometries by Carman (1956). Also, see the discussion by Ogushwitz (1985a).

Some investigators have expressed the virtual mass parameter m (see [7]) as $m = \alpha\rho_f/\phi$, where α is called the "structure factor" or the "tortuosity". The tortuosity is related to the virtual mass coefficient c by

$$c = (\alpha - 1)\phi\rho_f. \qquad [14]$$

By analogy with the virtual mass force on an isolated particle in a fluid, Berryman (1981) suggested that the tortuosity be expressed by the relation

$$\alpha = 1 - r\left(1 - \frac{1}{\phi}\right). \qquad [15]$$

He noted that the term $r = 1/2$ for an isolated spherical particle and $0 \leqslant r \leqslant 1$ for other ellipsoidal shapes.

Johnson (1980) showed that the value of the virtual mass coefficient at high frequency could be determined through measurement of the index of refraction of "fourth sound" when the porous medium is saturated with Helium II. Johnson *et al.* (1982) used this method to measure the tortuosity as a function of the porosity ϕ for spherical glass beads. They altered the porosity by sintering the beads.

METHOD OF BEDFORD *ET AL.* (1984)

To describe the method introduced by Bedford *et al.* (1984), we begin with the one-dimensional forms of [5a,b]:

$$(1-\phi)\rho_s\ddot{u}_s = P\frac{\partial^2 u_s}{\partial x^2} + Q\frac{\partial^2 u_f}{\partial x^2} - b(\dot{u}_s - \dot{u}_f) - c(\ddot{u}_s - \ddot{u}_f) \quad [16a]$$

and

$$\phi\rho_f\ddot{u}_f = Q\frac{\partial^2 u_s}{\partial x^2} + R\frac{\partial^2 u_f}{\partial x^2} + b(\dot{u}_s - \dot{u}_f) + c(\ddot{u}_s - \ddot{u}_f). \quad [16b]$$

Let us suppose that the solid constituent of the fluid-saturated porous medium is subjected to a *spatially uniform*, steady-state oscillatory motion, so that the displacement u_s is of the form

$$u_s = De^{i\omega t}, \quad [17]$$

where D is a prescribed real constant and ω is the frequency. The resulting steady-state motion of the fluid is of the form

$$u_f = \bar{U}e^{i\omega t}, \quad [18]$$

where $\bar{U}$ is a complex constant. By substituting these expressions for u_s and u_f into the Biot equation of motion for the fluid constituent [16b], we obtain the result

$$\phi\rho_f\omega\bar{U} = (ib - \omega c)(\bar{U} - D). \quad [19]$$

Note that the terms in [16b] containing Q and R vanish because the motion is spatially uniform. We can solve the complex equation [19] for the two real coefficients b and c:

$$b = \phi\rho_f\omega\,\mathcal{I}m\left[\frac{\tilde{U}}{(\tilde{U}-1)}\right], \quad c = -\phi\rho_f\,\mathcal{R}e\left[\frac{\tilde{U}}{(\tilde{U}-1)}\right], \quad [20]$$

where $\tilde{U} = \bar{U}/D$. We can solve these two equations for b and c as functions of frequency if we can determine $\bar{U}$ as a function of frequency.

Thus, determining b and c reduces to the solution of a steady-state boundary value problem in fluid mechanics: we subject the solid constituent of a porous medium to a rigid oscillatory motion and solve for the motion of the fluid in the pores. Let $\mathbf{u}$ be the displacement vector of the fluid. By averaging $\mathbf{u}$ over the pore volume v, we determine the fluid displacement u_f which appears in Biot's equations:

$$u_f = \frac{1}{v}\int_v (\mathbf{u}\cdot\mathbf{e}_1)\,dv, \quad [21]$$

where the vector $\mathbf{e}_1$ is a unit vector which specifies the direction of the imposed motion of the solid constituent. By expressing the steady-state motion of the fluid in the pore as $\mathbf{u} = \bar{\mathbf{u}}e^{i\omega t}$ and introducing [18] into [21], we obtain $\bar{U}$ as a function of frequency:

$$\bar{U} = \frac{1}{v}\int_v (\bar{\mathbf{u}}\cdot\mathbf{e}_1)\,dv. \quad [22]$$

In the case of straight cylindrical pores, the oscillatory motion of the pore fluid can be determined in closed form. Bedford *et al.* (1984) showed that in this case the value of the drag coefficient b obtained from their method agrees with the result obtained by Biot (1956b). For more complicated pore geometries, such as the pore volume of a granular material, it is necessary to use a numerical method to determine the oscillatory motion of the pore fluid. The present authors (Yavari & Bedford 1988) used the finite element method to determine the drag and virtual mass coefficients for several two-dimensional pore geometries. By comparing our results to cases for which closed-form results are available, we concluded that it is possible to obtain accurate values of the coefficients for the range of frequencies of interest in studies of the acoustics of porous media. In this work we extend our investigation to three-dimensional pore geometries.

THE MIXED FINITE ELEMENT FORMULATION

Our objective is to use the finite element method to determine the motion of a viscous, compressible fluid in the pore volume of a porous medium when the pore walls are subjected to a spatially uniform, oscillatory motion. We formulate the problem in terms of the components of the displacement vector of the fluid and a Lagrange multiplier related to the pressure. A formulation of this type is called a "mixed" finite element method (e.g. Carey & Oden 1983). The formulation we use was described in our two-dimensional study (Yavari & Bedford 1988) and in more detail by Yavari (1988). Here we merely summarize the formulation used in this study.

Under the assumptions of small displacements and small changes in pressure and density, we can express the steady-state forms of the linear momentum (Navier–Stokes) equation, the continuity equation and the boundary condition as

$$\left.\begin{aligned} \bar{A}\nabla^2\bar{\mathbf{u}} + \bar{B}\nabla(\nabla\cdot\bar{\mathbf{u}}) + \bar{\mathbf{u}} = 0 \\ \nabla\cdot\bar{\mathbf{u}} = \frac{-\bar{p}}{K_f} \end{aligned}\right\} \quad \text{in } \Omega,$$

$$\bar{\mathbf{u}} = D\mathbf{e}_1 \qquad \text{on } \Gamma_s, \tag{23}$$

where $\bar{\mathbf{u}}$ is the displacement vector of the fluid, Ω is the domain (volume) in which the solution is to be obtained, Γ_s is the part of the surface of Ω corresponding to the boundary between the fluid and solid constituents and $\bar{p}$ is the pressure of the fluid. The term K_f is the bulk modulus of the fluid. The terms $\bar{A}$ and $\bar{B}$ are defined by (Yavari & Bedford 1988)

$$\bar{A} = \frac{i\eta}{(\rho_f\omega)} \tag{24a}$$

and

$$\bar{B} = \frac{K_f}{(\rho_f\omega^2)} + \frac{i(\kappa + \frac{1}{3}\eta)}{(\rho_f\omega)}, \tag{24b}$$

where η, ρ_f and κ are the viscosity, density and bulk viscosity of the fluid.

The boundary value problem [23] can be expressed as an equivalent variational problem. We take the inner product of the first equation with a variation $\delta\bar{\mathbf{u}}$ and integrate over the domain. We enforce the second equation by introducing a Lagrange multiplier $\bar{\lambda}$ (see Yavari & Bedford 1988). The resulting variational formulation is

$$\int_\Omega \left[\bar{A}\nabla\bar{\mathbf{u}} : \nabla\delta\bar{\mathbf{u}} + (\nabla\cdot\bar{\mathbf{u}}\delta\bar{\lambda} + \bar{\lambda}\nabla\cdot\delta\bar{\mathbf{u}}) - \left(\frac{1}{\bar{B}}\right)\bar{\lambda}\delta\bar{\lambda} - \bar{\mathbf{u}}\cdot\delta\bar{\mathbf{u}}\right] dv = 0. \tag{25}$$

The Lagrange multiplier is related to the pressure by $\bar{p} = -K_f\bar{\lambda}/\bar{B}$.

We obtain a finite element approximation for $\bar{\mathbf{u}}$ by replacing the domain Ω in [25] by a discretized domain Ω_h. Our objective is to seek approximate solutions $\bar{\mathbf{u}}_h$ and $\bar{\lambda}_h$ which depend on the mesh size h of the discretized domain. We assume that the solution $\bar{\mathbf{u}}_h$ is contained in a subspace of $H^1(\Omega_h)$ and that the solution $\bar{\lambda}_h$ is contained in a subspace of $H^0(\Omega_h)$, where $H^n(\Omega_h)$ denotes the set of functions on Ω_h whose nth derivatives are square integrable. In terms of suitable finite element basis functions ("shape functions") Ψ_j and Θ_n, which are simple functions defined piecewise—element by element—over the discretized domain (the "mesh"), we can write the approximate solutions in the forms

$$\bar{\mathbf{u}}_h(\mathbf{x}) = \sum_j \Psi_j(\mathbf{x})\bar{\mathbf{U}}_j \tag{26a}$$

and

$$\bar{\lambda}_h(\mathbf{x}) = \sum_n \Theta_n(\mathbf{x})\bar{\Lambda}_n. \tag{26b}$$

The shape functions Ψ_i contain complete polynomials of degree $k \geqslant 1$ which are smooth enough to be members of the class $H^1(\Omega_h)$. The shape functions Θ_m contain complete polynomials of degree

$r \geqslant 0$ which need not be smooth but are members of the class $H^0(\Omega_h)$. The coefficients $\bar{U}_j$ and $\bar{\Lambda}_n$ (the nodal point values of the dependent variables) must be determined to obtain the solutions.

By substituting [26a,b] into the discretized form of [25], we obtain the linear system of equations

$$\begin{bmatrix} \bar{K}_{11} & \bar{K}_{12} \\ \bar{K}_{12}^{T} & \bar{K}_{22} \end{bmatrix} \begin{bmatrix} \bar{U} \\ \bar{\Lambda} \end{bmatrix} = 0, \qquad [27]$$

where

$$(\bar{K}_{11})_{ij} = \int_{\Omega_h} [\bar{A} \nabla \Psi_i : \nabla \Psi_j - \Psi_i \Psi_j] \, dv,$$

$$(\bar{K}_{12})_{in} = \int_{\Omega_h} [\nabla \cdot \Psi_i \Theta_n] \, dv$$

and

$$(\bar{K}_{22})_{mn} = \int_{\Omega_h} \left[-\left(\frac{1}{\bar{B}}\right) \Theta_m \Theta_n \right] dv. \qquad [28]$$

We calculate the terms in [27] one element at a time, obtaining the final formulation by summing the contributions of the elements. We solve the equation by applying the "essential" boundary conditions $\bar{U} = D\mathbf{e}_l$ on the pore boundaries (where the unit vector $\mathbf{e}_l$ defines the direction of the oscillatory motion), and applying periodic and symmetry boundary conditions where appropriate.

COMPUTATIONAL CONSIDERATIONS

Choosing an appropriate element (i.e. choosing the polynomials which describe the shape functions) is particularly important for mixed finite element approximations (e.g. Cary & Oden 1983). The nature of the pore geometries we considered suggested the use of tetrahedral elements. First, we tried a 10-node tetrahedron with a quadratic approximation for the displacements, a discontinuous linear approximation for the Lagrange multiplier $\bar{\lambda}_h$, and a 4-point integration rule (see Zienkiewicz 1977, pp. 172, 202). With this element we had limited success for two-dimensional problems, but it was overconstrained for the three-dimensional problems. We then tried using a discontinuous constant approximation for the Lagrange multiplier. This approach failed for two-dimensional problems and led to only moderate success for the three-dimensional problems.

Due to our lack of success with the tetrahedral element, we decided to use the very reliable 20-node brick element, which we show in figure 1 referred to a local cartesian coordinate system (ξ, η, ζ). Four brick elements make up a tetrahedron, as shown in figure 2. We used a 20-node brick element from the "serendipity" family of elements (Zienkiewicz 1977). We used a piecewise linear expression for the Lagrange multiplier $\bar{\lambda}_h$:

$$\Theta_1 = 1, \quad \Theta_2 = \xi, \quad \Theta_3 = \eta, \quad \Theta_4 = \zeta.$$

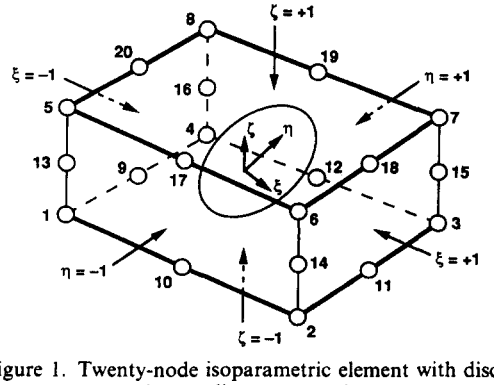

Figure 1. Twenty-node isoparametric element with discontinuous linear constraint.

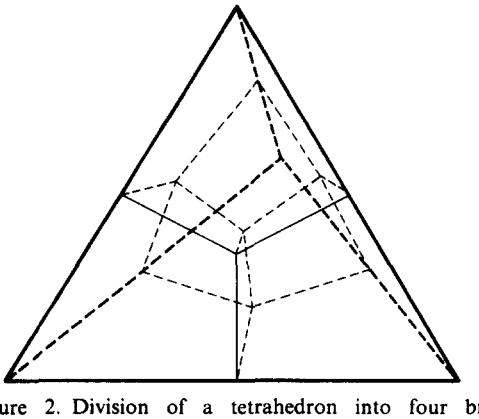

Figure 2. Division of a tetrahedron into four brick elements.

We used a quadratic expression for the displacement $\tilde{\mathbf{u}}_h$. The corner node values were

$$\Psi_i = \tfrac{1}{8}(1+\xi\xi_i)(1+\eta\eta_i)(1+\zeta\zeta_i)(\xi\xi_i+\eta\eta_i+\zeta\zeta_i-2)$$

and the typical mid-side node values were

$$\xi_i = 0, \quad \eta = \pm 1, \quad \zeta = \pm 1, \quad \Psi_i = \tfrac{1}{4}(1-\xi^2)(1+\eta\eta_i)(1+\zeta\zeta_i).$$

We used *isoparametric* elements to account for the curved geometries. We evaluated the integral terms in [27] by the 14-point quadrature rule, which accurately integrates up to the complete quintic polynomials (Irons 1971). The highest order polynomials involved in these expressions are fourth order (quadratic times quadratic). To solve the linear system of equations [27], we used a code based on the "frontal" method (Irons & Ahmad 1980).

THE MICROSTRUCTURE

For our first three-dimensional computations we chose a medium consisting of a face centered cubic (fcc) array of spherical grains [figure 3(a)]. The choice of an fcc packing to simulate a granular material was based in large part on our subjective judgment. We were unable to find information about natural packings of grains that would lead us to choose one packing over another. We were influenced by the fact that theoretical results exist for the elastic moduli of an fcc array of spherical grains. Thus our results would contribute to a complete evaluation of the coefficients in the Biot theory for this model material. The computed porosity of our finite element model of this medium was $\phi = 0.261$. [The exact porosity of an fcc packing of spheres is $1 - \pi/(3\sqrt{2}) = 0.2595$.] Due to the periodicity and symmetry of the packing, we only needed to model the motion of the fluid in one-fourth of the periodic element of the material [figure 3(b)].

From the finite element mesh we had designed to model the fcc array of spherical grains, we also obtained models for media consisting of fcc packings of 32-sided polyhedra. To investigate the effect of the porosity of the medium on the coefficients, we systematically altered the geometries of the polyhedra to obtain models of granular media having porosities $\phi = 0.480$, 0.431 and 0.382.

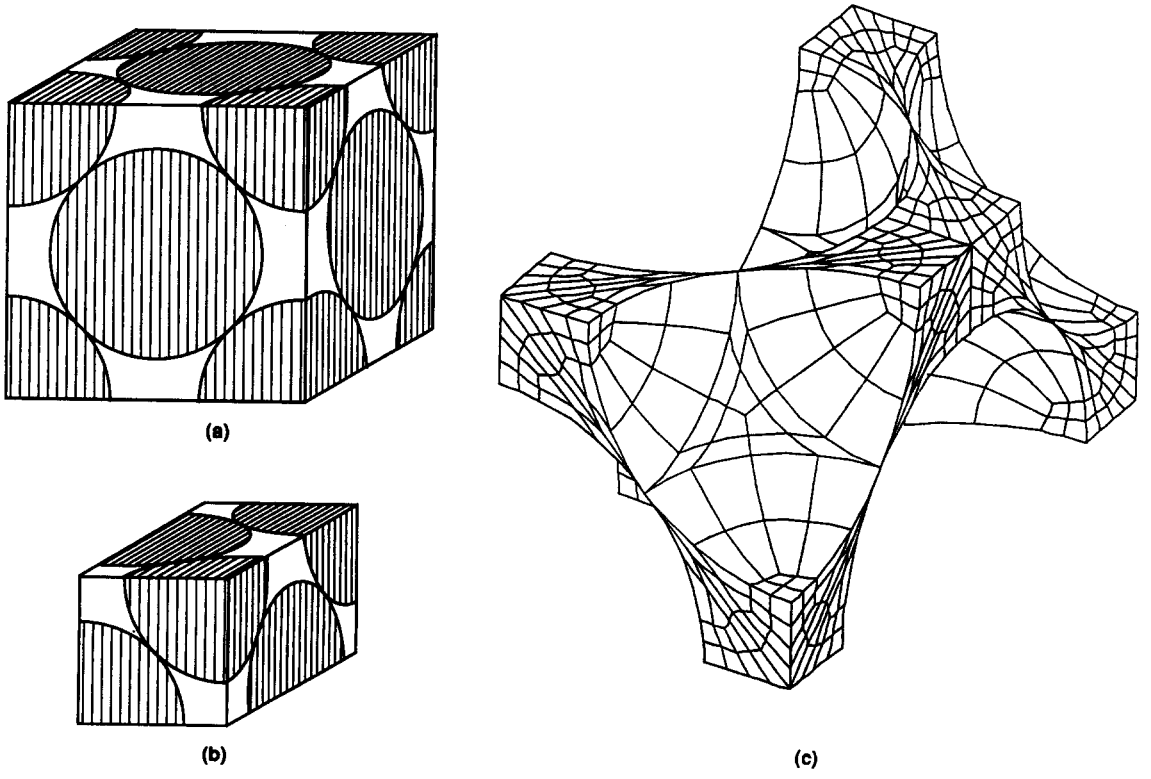

Figure 3. (a) An fcc packing of spherical grains. (b) The part of the periodic element needed for analysis. (c) The finite element mesh.

The pore volumes of the polyhedral media and the corresponding finite element meshes are shown in figures 4–6.

We first constructed course meshes of the pore spaces and then refined them to assess the accuracy of the solutions. For the spherical-grained medium and the polyhedral-grained medium with porosity $\phi = 0.480$, the course mesh had 192 elements and the refined mesh had 1536 elements. The refined mesh for the spherical-grained medium is shown in figure 3(c). The refined meshes for the three polyhedral-grained media are shown in figures 4(c), 5(c) and 6(c).

The maximum difference between the solutions we obtained using the course and refined meshes for the frequency range from $\omega = 100$ to 100,000 was 4% for the spherical-grained medium and 24% for the polyhedral-grained media. The results we report were obtained with the greatest refinement that was possible with our program and within the memory constraints of the Cray X-MP/24. Our numerical experiments with two-dimensional pore spaces for which exact solutions exist (Yavari & Bedford 1988) suggest that the errors in the three-dimensional results obtained with the refined mesh should be smaller than the differences between the results obtained with the course and the refined meshes.

RESULTS

In our two-dimensional study (Yavari & Bedford 1988), we showed that the coefficients b and c can be expressed in the functional forms

$$\frac{b}{\phi\rho_f\omega} = \mathscr{F}(\mathrm{Re}, \mathrm{M}), \quad \frac{c}{\phi\rho_f} = \mathscr{G}(\mathrm{Re}, \mathrm{M}),$$

where the dimensionless parameters Re and M are defined by

$$\mathrm{Re} = \frac{\rho_f\omega D^2}{\eta}, \quad \mathrm{M} = \frac{\omega D}{\left(\frac{K_f}{\rho_f}\right)^{1/2}}.$$

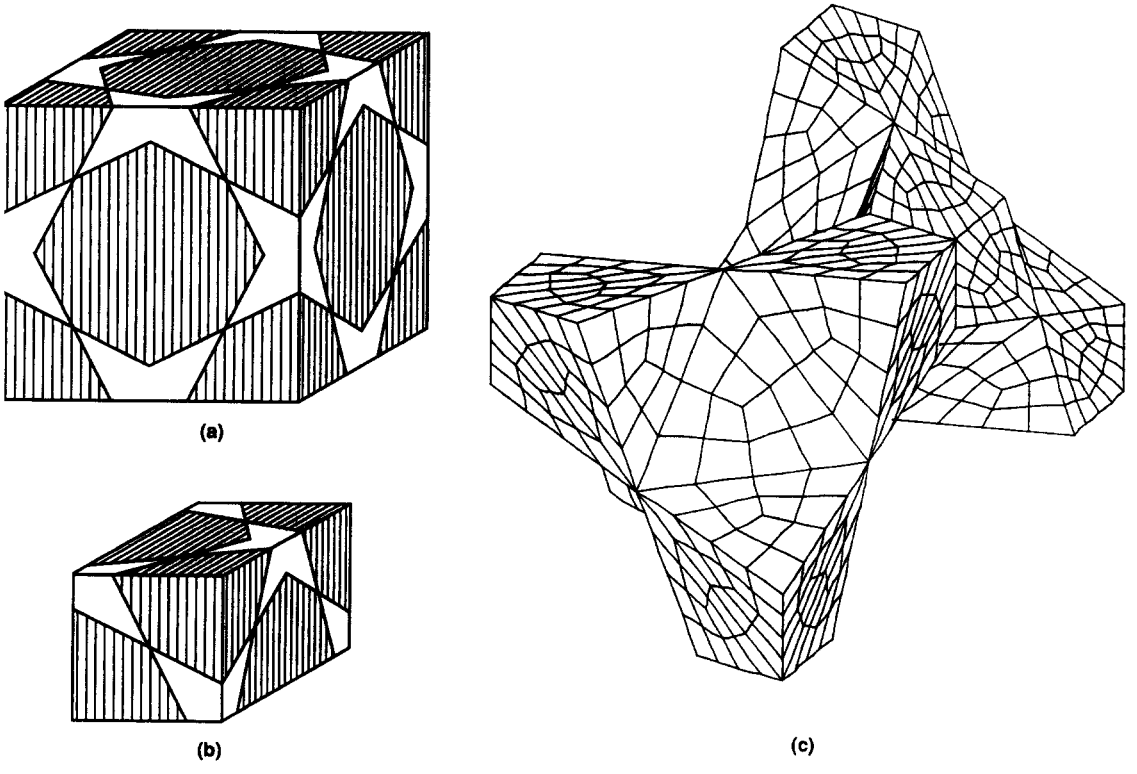

Figure 4. (a) An fcc packing of 32-sided polyhedral grains with porosity $\phi = 0.480$. (b) The part of the periodic element needed for analysis. (c) The finite element mesh.

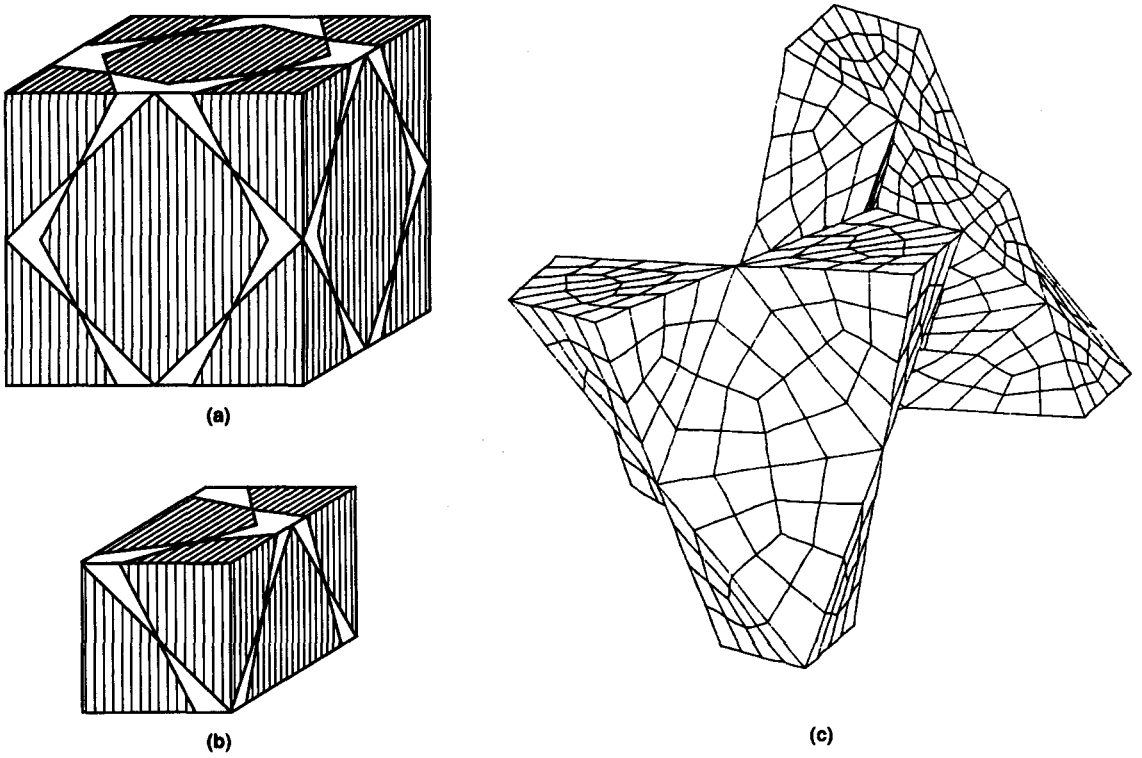

Figure 5. (a) An fcc packing of 32-sided polyhedral grains with porosity $\phi = 0.431$. (b) The part of the periodic element needed for analysis. (c) The finite element mesh.

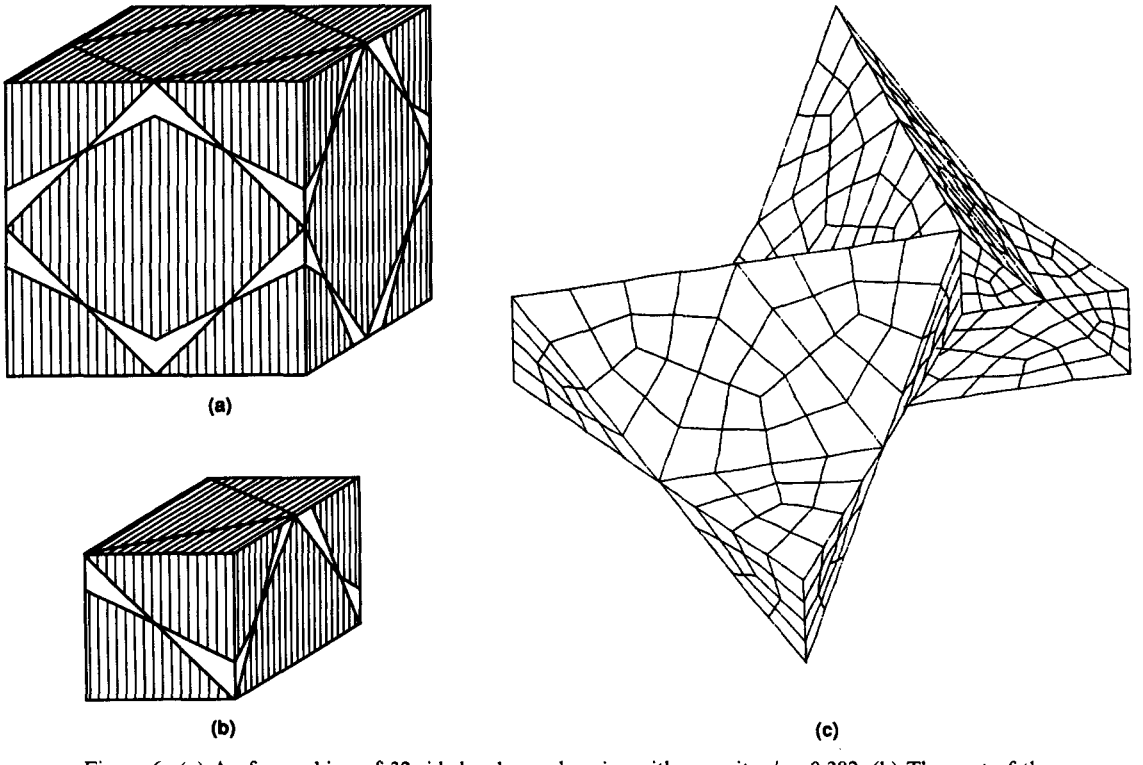

Figure 6. (a) An fcc packing of 32-sided polygonal grains with porosity $\phi = 0.382$. (b) The part of the periodic element needed for analysis. (c) The finite element mesh.

The terms η and K_f are the viscosity and bulk modulus of the fluid and D is a characteristic linear dimension of the pore volume. The parameters Re and M can be recognized as a Reynolds number and a Mach number, respectively. Re is the ratio of the frequency to the "critical" frequency, defined by Biot (1956b).

M is a measure of the effect of the compressibility of the fluid on the solutions for b and c. For frequencies that are sufficiently low that $M^2 \ll 1$, the effect of compressibility can be neglected and the quantities $b/(\phi\rho_f\omega)$ and $c/(\phi\rho_f)$ depend only on Re (Yavari & Bedford 1988). For this reason, we will present our results as plots of the dimensionless drag coefficient $b/(\phi\rho_f\omega)$ and dimensionless virtual mass coefficient $c/(\phi\rho_f)$ as functions of the dimensionless frequency Re. As a consequence, our results are independent of the properties of the fluid and the characteristic linear dimension D of the pore space as long as the restriction $M^2 \ll 1$ is satisfied. This condition requires that the characteristic linear dimension D be small compared to the wavelength.

In figures 7 and 8, we present the computed values of the nondimensional drag and virtual mass coefficients as functions of the dimensionless frequency Re. For the spherical grains, the characteristic linear dimension D is the sphere diameter. (The value we used in the computations was $D = 0.2$ mm.) For the polyhedral grains, the characteristic linear dimension D is the diagonal dimension of the faces of the computational elements shown in figures 4(b), 5(b) and 6(b).

By comparing the results shown in figures 7 and 8 to our results for various two-dimensional pore geometries (Yavari & Bedford 1988), we find that the qualitative behaviors of the dependence of b and c on the frequency are very similar for all of the pore geometries we have examined. In particular, the values of b and c are approximately constant (independent of the frequency) at low values of Re. In the case of a plane layer of fluid, the value of Re at which b and c are no longer independent of the frequency corresponds approximately to the value at which the thickness of the boundary layer at the wall of the layer of fluid extends across one-half the width of the layer. The boundary layer thickness $\delta = (2\nu/\omega)^{1/2}$, where $\nu = \eta/\rho_f$ is the kinematic viscosity of the fluid. By using this expression, we can write the nondimensional frequency in terms of the boundary layer thickness: $\mathrm{Re} = 2D^2/\delta^2$, where D is the width of the layer. From this result, we see that the boundary layer thickness is equal to one-half the width of the layer of fluid when $\mathrm{Re} = 8$.

Based on this result, we have arrived at a method for normalizing the results presented in figures 7 and 8. From figure 8, we estimated the value of frequency at which c was no longer constant for each of the three-dimensional pore geometries. By setting $\mathrm{Re} = \rho_f\omega D^2/\eta = 8$ for that value of frequency, we solved for D, obtaining an "effective gap size" for each geometry. The effective gap size we obtained in the case of the spherical grains was $D = 0.0448$ mm. For the polyhedral grains we obtained values of $D = 0.0479$, 0.0614 and 0.0758 mm for the porosities $\phi = 0.382$, 0.431 and 0.480, respectively. We then plotted the nondimensional drag and virtual mass coefficients as

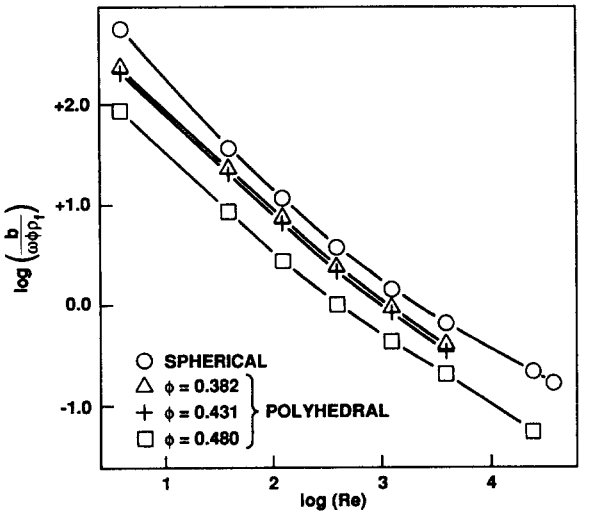

Figure 7. Computed values of $b/\omega\phi\rho_f$ as functions of $\mathrm{Re} = \rho_f\omega D^2/\eta$.

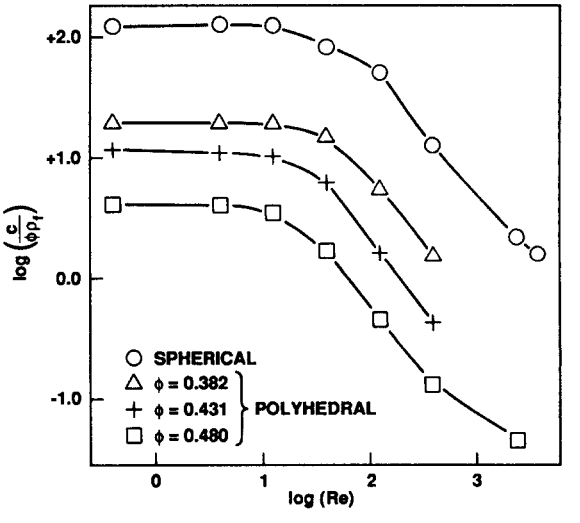

Figure 8. Computed values of $c/\phi\rho_f$ as functions of $\mathrm{Re} = \rho_f\omega D^2/\eta$.

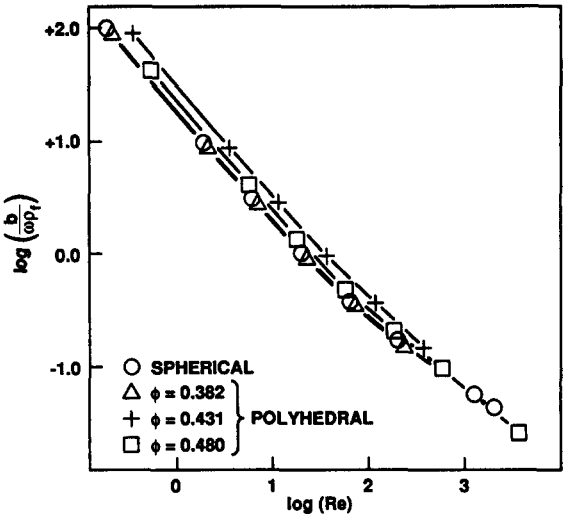

Figure 9. Computed values of $b/\omega\rho_f$ as functions of $\mathrm{Re} = \rho_f\omega D^2/\eta$ based on effective gap size.

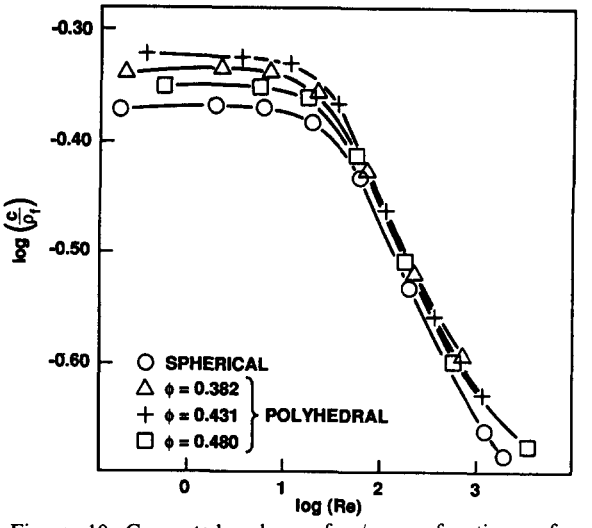

Figure 10. Computed values of c/ρ_f as functions of $\mathrm{Re} = \rho_f\omega D^2/\eta$ based on effective gap size.

functions of Re with Re based on the effective gap size. The results are shown in figures 9 and 10 as plots of $b/(\omega\rho_f)$ and c/ρ_f as functions of Re. (Notice that we have removed the porosity from the definitions of the nondimensional drag and virtual mass coefficients. We did so only because we observed that it led to a better normalization.) By comparing these plots to figures 7 and 8, we see that presenting the results in terms of effective gap size normalizes them reasonably well except for the virtual mass coefficient at low frequencies.

One of our motivations for carrying out this study was to compare our computed values of the drag and virtual mass coefficients for a three-dimensional pore volume with values based on Biot's solution for straight cylindrical pores (Biot 1956b). In figure 11 we compare our results for the drag coefficient b of an fcc stacking of spherical grains with [8]. We used [12] to evaluate the pore size parameter a_p. We used [13] to evaluate the permeability k_p with the empirical parameter k_0 set equal to 5 (see Carman 1956; Hovem & Ingram 1979; Ogushwitz 1985a). The agreement is excellent, which is consistent with our finding in our study of two-dimensional pore geometries (Yavari & Bedford 1988) that the drag coefficient is very insensitive to the pore geometry.

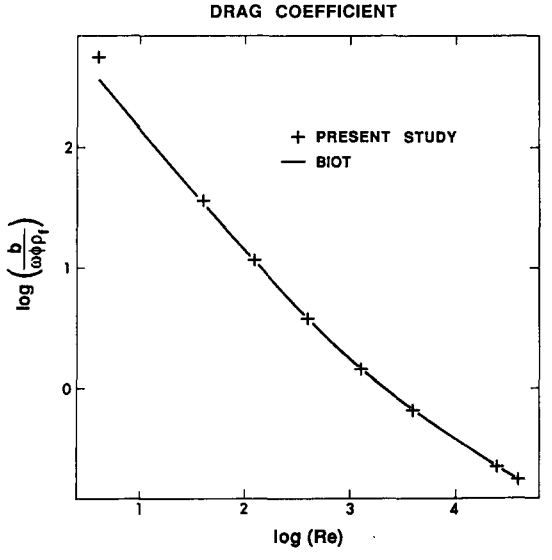

Figure 11. Comparison of computed values of $b/\phi\omega\rho_f$ as functions of $\mathrm{Re} = \rho_f\omega D^2/\eta$ with values based on Biot's result.

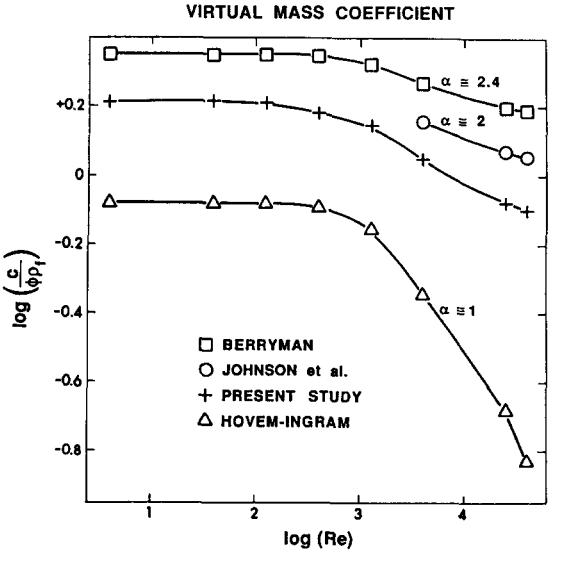

Figure 12. Comparison of computed values of $c/\phi\rho_f$ as functions of $\mathrm{Re} = \rho_f\omega D^2/\eta$ with values based on Biot's result.

In figure 12 we compare values of the virtual mass coefficient obtained using Biot's result with our results for spherical grains. In using Biot's result, Hovem & Ingram (1979) effectively assumed that the tortuosity $\alpha = 1$. Note that this assumption does not produce good agreement with our results. Results based on the value $\alpha = 2.4$, based on [15] (Berryman 1981), agree more closely with our results. We also show results obtained by choosing the value of the tortuosity to match the experimental measurement of the high frequency limit of the tortuosity by Johnson *et al.* (1982). From their data we estimated the value of the tortuosity for the porosity ($\phi = 0.261$) of our fcc packing of spherical grains to be $\alpha = 2$. Note that the results do not agree exactly with our computations. We see two possible reasons for the discrepancy. One is the difference between the stacking of the grains in their experiment and the fcc stacking we assumed in the computations. Another is that Johnson *et al.* sintered the beads to alter the porosity, which would have altered the pore geometry.

From figure 12 it is clear that our results for the virtual mass coefficient can be closely approximated by using an appropriate empirical choice for the tortuosity. Thus, we conclude that the empirical approach suggested by Biot (1956b) can adequately approximate our results for the frequency dependence of the drag and virtual mass coefficients for an fcc stacking of spherical grains.

Acknowledgements—This work was supported in part by the Office of Naval Research and the University of Texas Applied Research Laboratory. We thank John G. Heacock and Thomas A. Griffy for their encouragement and support. We are grateful to Professor Eric B. Becker of the University of Texas for advice on the finite element method and for permitting us to use his program TEXLESP-3D.

REFERENCES

AURIAULT, J.-L. 1980 Dynamic behavior of a porous medium saturated by a newtonian fluid. *Int. J. Engng Sci.* **18,** 775–785.

AURIAULT, J.-L. & SANCHEZ-PALENCIA, E. 1977 Étude du comportement macroscopique d'un mileu poreux saturé déformable. *J. Méc.* **16,** 575–603.

AURIAULT, J.-L., BORNE, L. & CHAMBON, R. 1985 Dynamics of porous saturated media. Checking of the generalized law of Darcy. *J. acoust. Soc. Am.* **77,** 1641–1650.

BEDFORD, A. 1986 Application of Biot's equations to a medium of alternating fluid and solid layers. *J. Wave–Mater. Interact.* **1,** 34–53.

BEDFORD, A., COSTLEY, R. D. & STERN, M. 1984 On the drag and virtual mass coefficients in Biot's equations. *J. acoust. Soc. Am.* **76,** 1804–1809.

BERRYMAN, J. G. 1980 Confirmation of Biot's theory. *Appl. Phys. Lett.* **37,** 382–384.

BERRYMAN, J. G. 1981 Elastic wave propagation in fluid-saturated porous media. *J. acoust. Soc. Am.* **69,** 416–424.

BIOT, M. A. 1956a Theory of elastic waves in a fluid saturated porous solid, I. Low frequency range. *J. acoust. Soc. Am.* **28,** 168–178.

BIOT, M. A. 1956b Theory of elastic waves in a fluid saturated porous solid, II. Higher frequency range. *J. acoust. Soc. Am.* **28,** 179–191.

CAREY, G. F. & ODEN, J. T. 1983 *Finite Elements*; Vol. II, *A Second Course.* Prentice-Hall, Englewood Cliffs, N.J.

CARMAN, P. C. 1956 *Flow of Gases through Porous Media.* Academic Press, New York.

HOVEM, J. M. & INGRAM, J. D. 1979 Viscous attenuation of sound in saturated sand. *J. acoust. Soc. Am.* **66,** 1807–1812.

IRONS, B. M. 1971 Quadrature rules for brick-based finite elements. *Int. J. numer. Meth. Engng* **3,** 293–294.

IRONS, B. & AHMAD, S. 1980 *Techniques of Finite Elements*, pp. 203–252. Horwood, Chichester, West Sussex.

JOHNSON, D. L. 1980 Equivalence between fourth sound in liquid He II at low temperatures and the Biot slow wave in porous media. *Appl. Phys. Lett.* **37,** 1065–1067.

JOHNSON, D. L. & PLONA, T. J. 1982 Acoustic slow waves and the consolidation transition. *J. acoust. Soc. Am.* **72,** 556–565.

JOHNSON, D. L. & PLONA, T. J., SCALA, C., PASIERB, F. & KOJIMA, H. 1982 Tortuosity and acoustic slow waves. *Phys. Rev. Lett.* **49,** 1840–1844.

OGUSHWITZ, P. R. 1985a Applicability of the Biot theory. I. Low-porosity materials. *J. acoust. Soc. Am.* **77,** 429–452.

OGUSHWITZ, P. R. 1985b Applicability of the Biot theory. II. Suspensions. *J. acoust. Soc. Am.* **77,** 440–441.

STOLL, R. D. 1974 Acoustic waves in saturated sediments. In *Physics of Sound in Marine Sediments* (Edited by HAMPTON, L. D.), pp. 19–39. Plenum Press, New York.

STOLL, R. D. 1977 Acoustic waves in ocean sediments. *Geophysics* **42,** 179–191.

STOLL, R. D. & BRYAN, G. M. 1969 Wave attenuation in saturated sediments. *J. acoust. Soc. Am.* **47,** 1440–1447.

YAVARI, B. 1988 Micro-mechanics of granular fluid saturated porous media using the finite element method. Ph.D. Dissertation, Univ. of Texas at Austin.

YAVARI, B. & BEDFORD, A. 1988 Computation of the Biot drag and virtual mass coefficients. *Int. J. Multiphase Flow* **14,** 1–12.

ZIENKIEWICZ, O. C. 1977 *The Finite Element Method*, 3rd edn, pp. 155–160. McGraw-Hill, London.